To appear in: Environmental Fluid Mechanics

Noname manuscript No.
(will be inserted by the editor)

Periodically driven circulation near the shore of a lake

Duncan E. Farrow

the date of receipt and acceptance should be inserted later

Abstract Solutions are found for a linear model of the circulation near the shore of a lake that is subject to two diurnal forcing mechanisms. The first is the day/night heating/cooling induced horizontal pressure gradient. The second is an unsteady surface stress modelling a sea breeze/gully wind pattern. The two forcing mechanisms can oppose or reinforce each other depending on their relative phase. The interplay of different dynamic balances at different times and locations in the domain lead to complex circulation patterns especially during the period of flow reversal.

1 Introduction

The fluid dynamics of surface water bodies has motivated a large number of investigations into flow in shallow cavities. The flow can be driven by any combination of mechanisms and effects such as differential heating, topography and surface stress. The now classic cubic velocity profile for convection driven by a horizontal density gradient was apparently first derived by Rattray & Hansen [17] in their study of estuarine circulation. The asymptotic series solution for steady convection in shallow rectangular cavity driven by end walls at different temperatures considered by Cormack, Leal & Imberger [1] shows this cubic velocity profile. The analytical results in [1] were confirmed experimentally by Imberger [9] and numerically by Cormack, Leal & Seinfeld [2]. The results of [1] where generalised to include a surface stress by Cormack, Stone & Leal [3] who found that quite a small surface stress could dominate the velocity structure and hence the horizontal heat transfer in the cavity.

All of the studies mentioned above have been for steady flow in a rectangular cavity. For many geophysical flows, for example circulation near the shore of a lake, a variable or

D. E. Farrow
Mathematics & Statistics
Murdoch University
Murdoch WA 6150
Australia
Tel.: +61 8 9360 2819
Fax: +61 8 9360 6332
E-mail: D.Farrow@murdoch.edu.au

sloping bathymetry is more appropriate. Furthermore, the unsteady nature of the thermal or surface stress forcing means that the circulation does not achieve steady state conditions before there is a significant change in the magnitude or nature of the forcing [16,5]. This has motivated several studies of unsteady flow in non-rectangular domains modelling daytime heating, nighttime cooling or both.

The daytime heating phase of the diurnal cycle has been subject to several recent investigations following on from the early asymptotic results of Farrow & Patterson [7]. Lei & Patterson [10] present a detailed scaling analysis with accompanying numerical results that elucidate many of the possible flow regimes. Mao, Lei & Patterson [15] revisited and generalised these results. The secondary circulation induced by the bottom boundary heating that occurs during the day was investigated by Farrow & Patterson [6] and more recently by Mao, Lei & Patterson [13]. These results showed a complex interplay between the attenuation length of the incoming radiation and the local depth leading to several possible flow regimes.

Numerical modelling of the nighttime cooling phase was carried out by Horsh, Stefan & Gavali [8] where the flow includes both overturning and a down-slope flow. There has been more recent scaling and numerical modelling by Lei & Patterson [11] and Mao, Lei & Patterson [14]. The scaling and numerical results identified a number of possible flow regimes with distinctive sub-regions. The bottom slop was a crucial parameter.

Farrow & Patterson [5] and Farrow [4] used asymptotic and numerical methods to consider a combined heating/cooling cycle. In this work the primary focus was the unsteady flow response to the unsteady forcing. It was found that, in the shallow cavity case, the response depended on the local depth with viscous/buoyancy balance dominating in the shallows and an unsteady inertial/buoyancy balance dominating in the deeper parts of the domain. This latter balance in those asymptotic results essentially represents a balance between the u_t and pressure gradient terms in the momentum equations. Lei & Patterson [12] included a more general heating/cooling model and geometry in their numerical investigation of the diurnal cycle. Their results of the overall flow structure have qualitative features in common with the vertically integrated models [5,4] but brought out interesting detailed differences between the dynamics of the daytime and nighttime parts of the diurnal cycle.

As noted above [3] found that a relatively small surface stress could have a large impact on the circulation and transport in a shallow cavity. The aim of this paper is to generalise the unsteady solutions of [5] to include the effects of a surface stress. The surface stress is assumed to be periodic modelling a sea breeze/gully wind pattern commonly found in coastal regions.

This paper formulates a linear model of periodically forced circulation in the near shore regions of a lake. The circulation is due to two forcing mechanisms. Following [5,4] the first is a vertically integrated heating/cooling term modelling the diurnal heating/cooling cycle. The second is a periodic surface stress boundary condition applied at the upper surface of the water body. This models a typical sea breeze/gully wind system where the wind direction changes during the daily cycle. The two forcing mechanisms will not necessarily be in phase and the model is used to investigate the influence of the relative phase of the two mechanisms on the circulation structure.

2 Model Formulation

The near shore circulation in a lake is modelled by the flow of a viscous fluid contained in the wedge $-Ax < z < 0$ in the (x,z)-plane where A is the bottom slope of the region. The

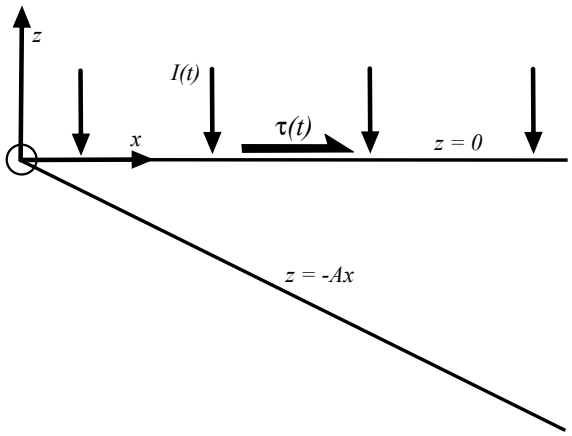

Fig. 1 Schematic of flow domain and coordinate system.

flow domain is shown in Figure 1. Typically A is a small parameter which means that the circulation can be assumed to be hydrostatic and horizontal diffusion can be neglected. For the purposes of the model here non-linear advection terms are also neglected.

The circulation is driven by two mechanisms. The first is a diurnal heating/cooling cycle (discussed below) and the second is a diurnal surface stress $\tau(t)$ (defined below).

The circulation is then modelled by the system

$$\frac{\partial u}{\partial t} = -\frac{1}{\rho_0}\frac{\partial p}{\partial x} + \nu\frac{\partial^2 u}{\partial z^2} \tag{1}$$

$$0 = -\frac{1}{\rho_0}\frac{\partial p}{\partial z} + g\alpha(T - T_0) \tag{2}$$

$$\frac{\partial T}{\partial t} = \kappa\frac{\partial^2 T}{\partial z^2} + H(x,z,t) \tag{3}$$

$$\frac{\partial u}{\partial x} + \frac{\partial w}{\partial z} = 0 \tag{4}$$

where u and w are the fluid velocities in the x and z directions respectively, t is time, p is the pressure perturbation, T is the temperature, ρ_0 is the reference density (at reference temperature T_0), ν is the kinematic viscosity, κ is the thermal diffusivity, g is the gravitational acceleration constant, α is the coefficient of thermal expansion, C_p is the specific heat of water and $H(x,z,t)$ is a heating/cooling term that encapsulates the diurnal cycle (discussed below). The above system of equations are to be solved subject to the boundary and initial conditions

$$\rho_0\nu\frac{\partial u}{\partial z} = \tau_0\sin(2\pi(t/P - \phi)),\ w = 0,\ \frac{\partial T}{\partial z} = 0 \quad \text{on } z = 0 \tag{5}$$

$$u = w = 0,\ \frac{\partial T}{\partial z} = 0 \quad \text{on } z = -Ax \tag{6}$$

$$u = w = 0,\ T = T_0 \quad \text{at } t = 0 \tag{7}$$

where τ_0 is the magnitude of the surface stress and $\phi \in [0,1]$ is a constant that parameterises the phase difference between the two forcing mechanicsms.

The formulation of the heating/cooling therm in (3) is as follows. Following earlier modelling of the diurnal cycle [5,4] it is assumed that a surface heat flux of magnitude $I(t) = I_0 \cos(2\pi t/P)\mathrm{Wm}^{-2}$ (where P is the period of a day and I_0 is the maximum heat flux) is distributed uniformly over the local depth. Vertically integrating the heat transfer is a considerable simplification of the thermal forcing mechanisms operant in natural lakes. For example, during the day most heating occurs near the surface with relatively little penetrating the full depth of the lake [7,10,15]. At night, surface cooling leads to penetrative convection that leads to approximately vertically uniform cooling [8,14]. However, to allow feasible analytic progress and to reduce the number of modelling parameters the simpler vertically integrated model is used here. This leads to a heating/cooling term that is independent of z given by

$$H(x,t) = \frac{I_0}{\rho_0 C_p A x} \cos(2\pi t/P). \tag{8}$$

The diurnal heating/cooling appears as a forcing term in (3) while the periodic stress appears in the boundary condition (5). Both forcing mechanisms assume a purely sinusoidal form for the time variation. Since the model below is linear more complicated periodic behaviour could be examined using Fourier series however this is beyond the scope of the present work.

The model equations do not include any non-linear (specifically advection) terms. This is a considerable simplification of the dynamics that apply in natural lakes and thus limits the applicability of the model. Despite these limits the model does show some interesting features and dynamics of the circulation. Making analytical progress is also difficult when non-linear terms are included.

The model equations are now non-dimensionalised using the scales [4]

$$t \sim P,\ z \sim H = \sqrt{\nu P},\ x \sim H/A,\ T - T_0 \sim I_0 P/(\rho_0 C_p H),$$
$$u \sim AU,\ w \sim A^2 U \text{ and } p \sim g\alpha I_0 P/C_p \tag{9}$$

where the generic velocity scale U is given by

$$U = \frac{g\alpha I_0 P^2}{\rho_0 C_p H}. \tag{10}$$

The model equations then become

$$u_t = -p_x + u_{zz} \tag{11}$$
$$0 = -p_z + T \tag{12}$$
$$T_t = \frac{1}{\sigma} T_{zz} + \frac{1}{x}\cos(2\pi t) \tag{13}$$
$$u_x + w_z = 0 \tag{14}$$

where $\sigma = \kappa/\nu$ is the Prandtl number of water and all variables are now dimensionless. The boundary and initial conditions become

$$u_z = S\sin(2\pi(t-\phi)),\ w = T_z = 0 \quad \text{on } z = 0 \tag{15}$$
$$u = w = T_z = 0 \quad \text{on } z = -x \tag{16}$$
$$u = w = T = 0 \quad \text{at } t = 0 \tag{17}$$

where

$$S = \frac{\tau_0 C_p}{Ag\alpha I_0 P} \tag{18}$$

is a dimensionless quantity representing the relative magnitude of surface stress to buoyancy forces.

This is effectively now a two parameter problem (σ does not appear in the solution below) with S a measure of the relative magnitude of surface stress to buoyancy forcing and ϕ characterising the relative phase of the two forcing mechanisms. If $\phi = 0$ then the two mechanisms are in phase and working in concert. If $\phi = \frac{1}{2}$ the the two forcing mechanisms are exactly out of phase and opposing each other.

The temperature equation can be solved independently of the momentum equations. Moreover, since the forcing term is independent of z and the boundary conditions are insulated the solution is independent of z and is given by

$$T(x,t) = \frac{1}{2\pi x}\sin(2\pi t). \tag{19}$$

Solving for u involves eliminating the pressure and using a stream function formulation. The details are omitted however the solution for $u(x,z,t)$ can be written as

$$u(x,z,t) = u_B(x,z,t) + Su_S(x,z,t) \tag{20}$$

where

$$\begin{aligned} u_B(x,z,t) = &-\frac{1}{96\pi x^2}\sin(2\pi t)(z+x)(8z^2+zx-x^2) \\ &-2x\sum_{n=1}^{\infty}\frac{\cos\beta_n + (\cos\beta_n - 1)/\beta_n^2 - \frac{1}{2}}{\beta_n^3\sin\beta_n((\beta_n/x)^4+(2\pi)^2)}(\cos(\beta_n z/x)-\cos\beta_n) \\ &\times\left((\beta_n/x)^2(\cos(2\pi t)-\exp(-(\beta_n/x)^2 t)) + 2\pi\sin(2\pi t)\right) \end{aligned} \tag{21}$$

and

$$\begin{aligned} u_S(x,z,t) = &\frac{2}{x}\sum_{n=1}^{\infty}\frac{\left((1+\beta_n^2)\cos\beta_n - 1\right)\cos(\beta_n z/x)+\cos\beta_n}{\beta_n\sin\beta_n(4\pi^2+(\beta_n/x)^2)} \\ &\times\left[(\beta_n/x)^2\sin(2\pi(t-\phi)) - 2\pi\cos(2\pi(t-\phi))\right. \\ &\left.+\exp(-(\beta_n/x)^2 t)[(\beta_n/x)^2\sin(2\pi\phi)+2\pi\cos(2\pi\phi)]\right] \end{aligned} \tag{22}$$

where β_n are the positive roots of $\beta_n = \tan\beta_n$. Physically, u_B is the flow associated with buoyancy forcing only [5] (i.e. $S = 0$) and u_S is the flow when no buoyancy effects are present. Since the model is linear these solutions simply add when both effects are present. Also, as $t \to \infty$ the solutions become purely periodic in nature.

The solutions above include both viscous and unsteady inertial effects. In the shallows (as $x \to 0$) unsteady inertial effects can be neglected which yields the limiting cases

$$u_B \to u_{Bv} = \frac{x}{96\pi}\left(\frac{z}{x}+1\right)\left(8\left(\frac{z}{x}\right)^2+\frac{z}{x}-1\right)\sin(2\pi t) \tag{23}$$

and

$$u_S \to u_{Sv} = x\left(\frac{z}{x}+1\right)\sin(2\pi(t-\phi)) \tag{24}$$

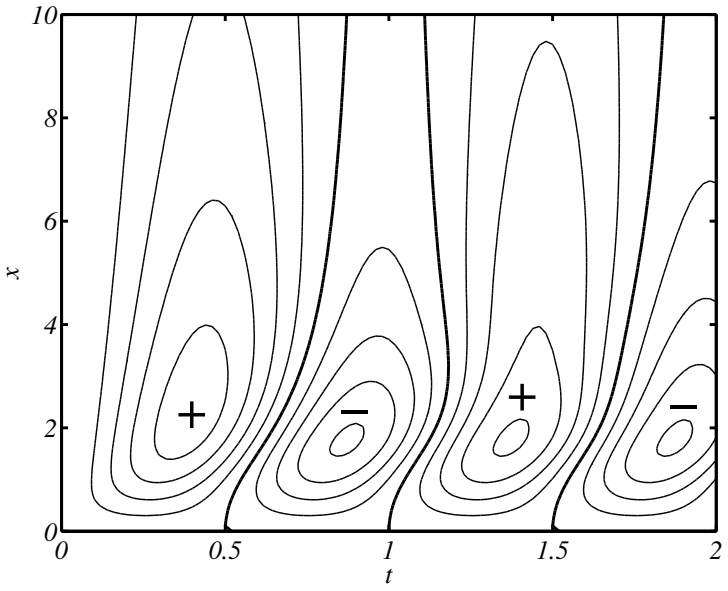

Fig. 2 Contours of the surface velocity $u|_{z=0}$ in the (t,x)-plane for the case $S=0$. The heavy contour is the zero contour indicating a stagnation point on the surface. The contour interval is 10^{-3} and the $+$ and $-$ signs indicate the sign of the velocity.

as $x \to 0$. These two solutions are essentially modulated equivalents of the steady-state solutions of [3]. Note that u_{Sv} does not in general satisfy the initial condition since the unsteady u_t term has been neglected in the governing equations. There is a large x (inviscid) limit for u_B which is obtained by neglecting viscous effects:

$$u_B \to u_{Bi} = \frac{1}{4\pi^2 x}\left(\frac{z}{x}+\frac{1}{2}\right)(1-\cos(2\pi t)). \tag{25}$$

Note that this is just a linear velocity profile and does not satisfy the boundary conditions at $z=0$ and $z=-x$. As $x \to \infty$ u_S tends to the infinite depth solution which (for large times after transient terms have disappeared) is given by

$$u_S \to u_{S\infty} = \frac{1}{(2\pi)^{1/2}}\exp\left(\pi^{1/2}z\right)\sin\left(2\pi\left(t-\phi-\frac{1}{8}\right)+\pi^{1/2}z\right). \tag{26}$$

In this limit the flow is mainly in a layer near $z=0$ with the magnitude of u_{Sv} decaying exponentially with depth.

3 Discussion

3.1 Introductory Remarks

The solution given in (20) has two obvious limits: the surface stress dominated case $S \gg 1$ and the buoyancy dominated case $S \ll 1$ The latter buoyancy dominated case has been

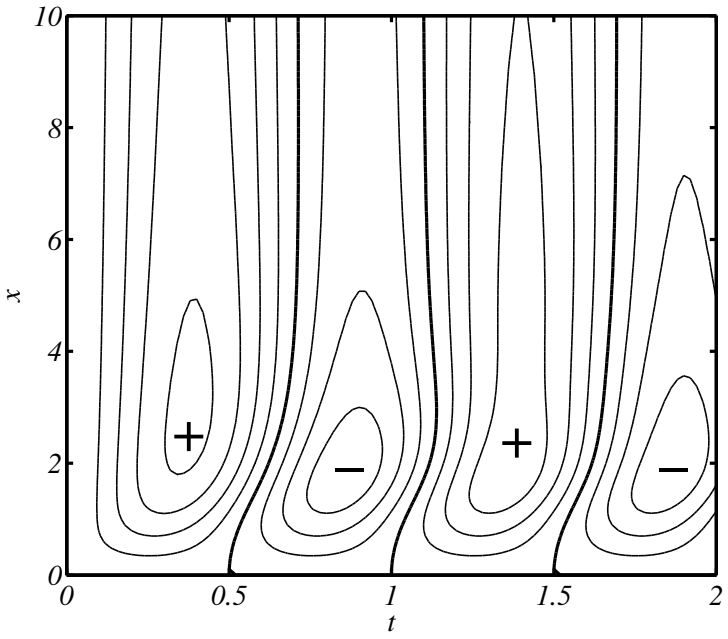

Fig. 3 Contours of the surface velocity $u|_{z=0}$ in the (t,x)-plane for the case $S = 0.01$ and $\phi = 0$. The heavy contour is the zero contour indicating a stagnation point on the surface. The contour interval is 2×10^{-3} and the $+$ and $-$ signs indicate the sign of the velocity.

considered in detail previously [5,4]. Those results can be summarised by considering the surface velocity $u|_{z=0}$ for $S = 0$ since the surface velocity generally indicates the sense of the circulation at depth. Contours of the surface velocity for $S = 0$ in the (t,x)-plane are shown in Figure 2. The contours show the transition from the viscous dominated shallow region $x < 1$ where the circulation is in phase with the forcing (as in the viscous limit solution (23)) to the deeper unsteady inertia dominated flow where the circulation lags the forcing by up to half a period during the early adjustment times. The reversal of the circulation is characterised by either an upwelling front (day to night transition) or a down welling front (night to day transition) emanating from the shore at $x = 0$ and moving out into the domain. Other points are that for small x the magnitude of $u \sim x$ while as $x \to \infty$ the magnitude of $u \sim x^{-1}$. Finally, after an initial adjustment time that is proportional to $\sqrt{x}$ the flow is purely periodic with reversal of the circulation in the deeper parts of the domain lagging the reversal of the forcing by a quarter of a period.

The surface stress dominated case is not particularly interesting and is only discussed briefly here. The overall qualitative structure of the surface stress dominated case is not much different from the buoyancy dominated case. For small x the magnitude of $u \sim x$ but for large x the magnitude of u tends to a finite value. Also, for large x the magnitude of the velocity associated with the surface stress decays exponentially with depth and in this limit the reversal of the circulation lags the change in the sign of the surface stress by $1/8$ of a period (see (26)).

The decay of u_S with depth means that the circulation in the sufficiently deep parts of the domain will be dominated by buoyancy forcing even for large values of S since in this

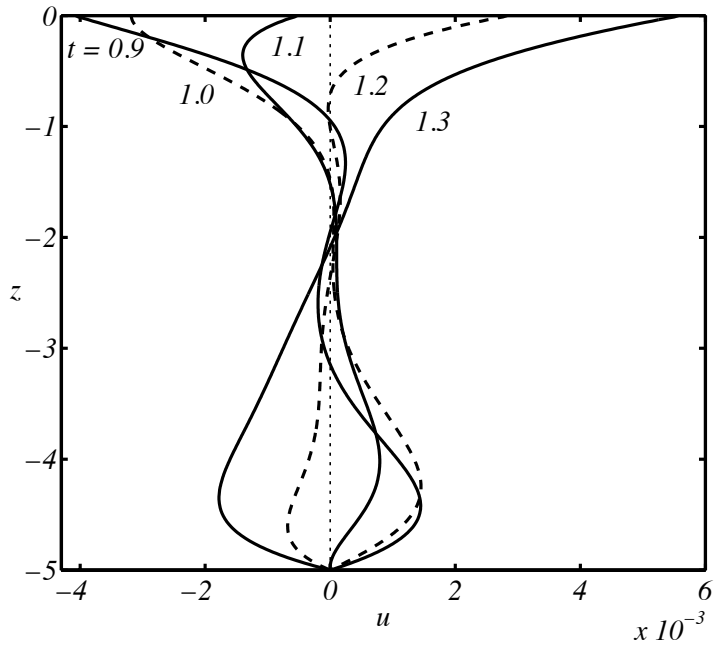

Fig. 4 Velocity profiles for $S = 0.01$ and $\phi = 0$ at $x = 5$ for various times as the circulation changes direction.

thermally vertically integrated model, buoyancy effects penetrate the entire depth of the domain.

The discussion that follows concentrates on the most interesting case where the buoyancy and surface stress forcing are of similar magnitude. When buoyancy and surface stress are of similar magnitude the parameter of interest is then ϕ the phase difference between the two forcing mechanisms. When $\phi = 0$ the forcing mechanisms are exactly in phase and reinforce each other while when $\phi = \frac{1}{2}$ the forcing mechanisms are exactly out of phase and act counter to each other.

3.2 Forcing mechanisms are in phase: $\phi = 0$

Figure 3 shows contours of the surface velocity $u|_{z=0}$ in the (t,x)-plane for $S = 0.01$ and $\phi = 0$. Here, the two forcing mechanisms are in phase. There is little qualitative change in the figure compared with the $S = 0$ case (Figure 2) except for an overall increase in magnitude (by a factor of about 2) and some change in location of the contours, especially for larger x. The approximate doubling in magnitude is due to both forcing mechanisms working in concert while the difference in position of the contours is due to the surface stress forcing dominating the buoyancy forcing for large x. Otherwise the $\phi = 0$ case is qualitatively similar to the buoyancy only case with the viscous dominated flow near $x = 0$ being in phase with the forcing while the flow in the deeper parts shows a lag in the flow reversal due to unsteady inertial effects.

Figure 4 shows some velocity profiles at $x = 5$ for various times as a flow reversal takes place. The vertical structure of the profiles can be broken into three regimes. Firstly, near

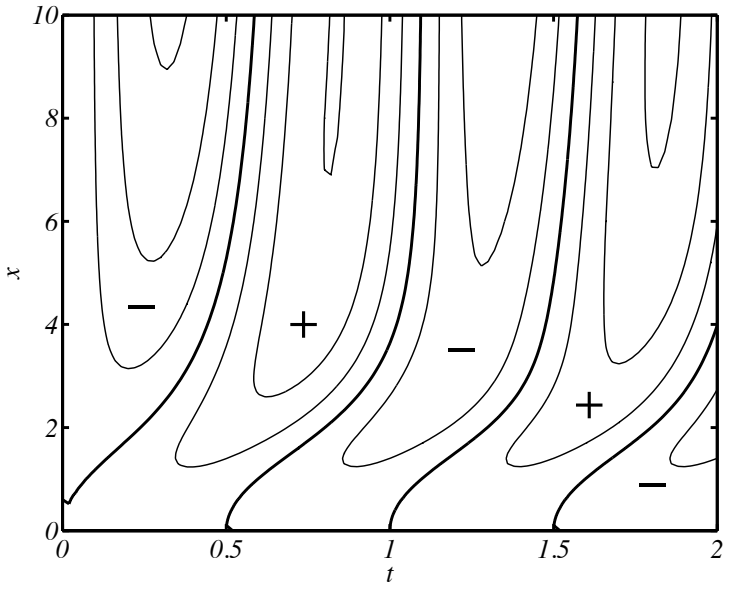

Fig. 5 Contours of the surface velocity $u|_{z=0}$ in the (t,x)-plane for the case $S = 0.01$ and $\phi = \frac{1}{2}$. The heavy contour is the zero contour indicating a stagnation point on the surface. The contour interval is 10^{-3} and the $+$ and $-$ signs indicate the sign of the velocity.

the surface $z = 0$ the flow is dominated by the surface stress boundary condition. Secondly, at intermediate depths the main balance is between buoyancy and unsteady inertia and there is little influence felt by the surface stress boundary condition. Thirdly there is a boundary layer near $z = -5$ where a viscosity/buoyancy balance applies. The reversal of both forcing mechanisms (from night to day) occurs at $t = 1.0$. At $t = 0.9$ the existing nighttime flow is visible near the surface (where $u < 0$) and in the bottom boundary layer (where $u > 0$). However, in the intermediate depths ($-3 < z < -1$) the circulation is clockwise which is indicative of a daytime flow structure. The circulation at intermediate depths is a result of the inertia of the previous daytime circulation (established during $0 < t < 0.5$) persisting against the nighttime buoyancy forcing. Within the viscous boundary layers near $z = -5$ and $z = 0$ the flow responds quickly to changes to forcing and thus at $t = 0.9$ the flow in these regions reflect the nighttime structure. These effects lead to the velocity profile at $t = 0.9$ having four distinct layers. As time progresses ($t = 1.0$ to 1.3) the flow in the viscous dominated regions rapidly respond to the change to daytime forcing conditions. Since the flow at intermediate depths already has a daytime structure the circulation in that region accelerates as time progresses. Note that at $t = 1.3$ the velocity profile at intermediate depths is close to linear as predicted by an unsteady inertia/buoyancy balance although the magnitude differs slightly from that predicted by (25) since the effects of viscosity and the surface stress boundary condition are not entirely absent. It should be noted that the effects of the surface stress boundary condition decay with depth and do not penetrate the full depth of the water column. This is in contrast to the steady-state results of Cormack, Stone & Leal [3] where the effects of the surface stress are felt over the entire depth.

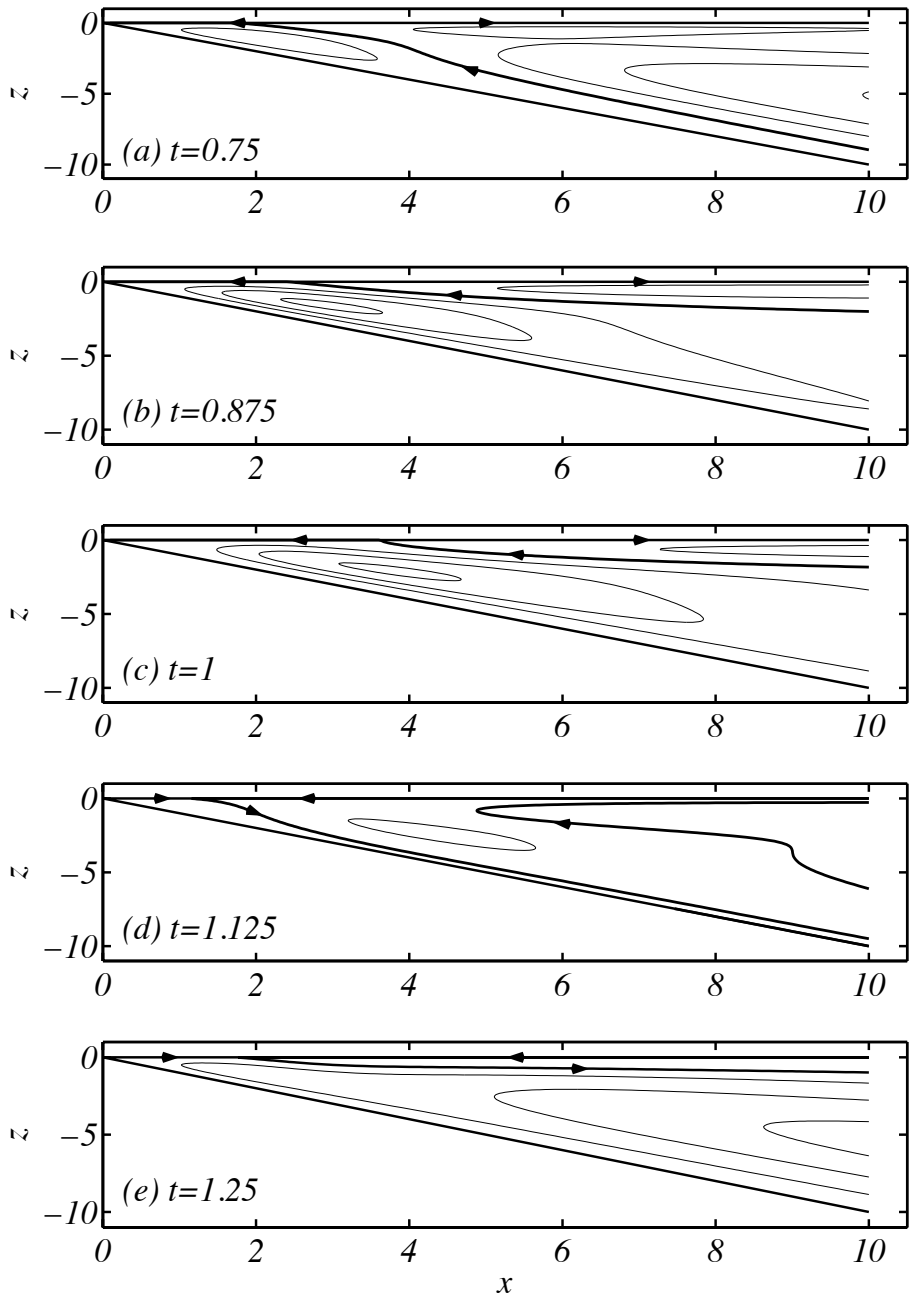

Fig. 6 Streamlines at various times from the $S = 0.01$ and $\phi = \frac{1}{2}$ case. The heavy streamline is the zero streamline and the contour interval is 5×10^{-4}.

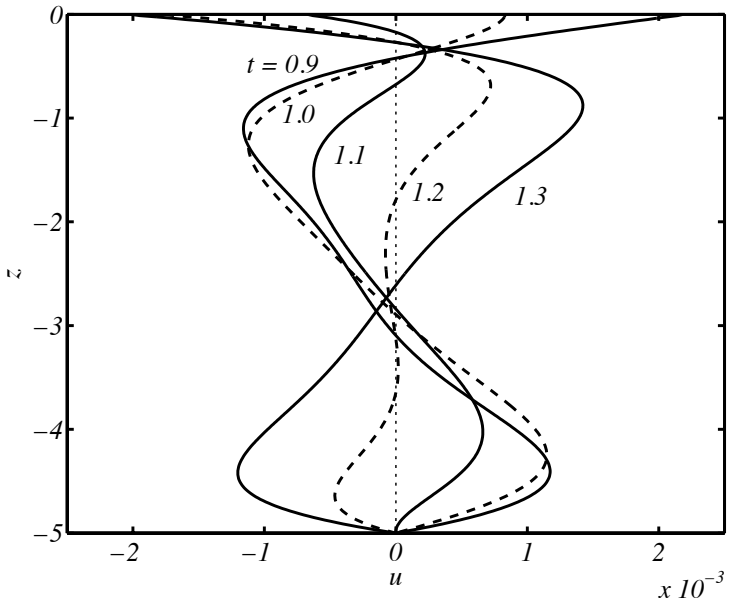

Fig. 7 Velocity profiles for $S = 0.01$ and $\phi = \frac{1}{2}$ at $x = 5$ for various times as the circulation changes direction.

3.3 Forcing mechanisms out of phase: $\phi = \frac{1}{2}$

In this case the two forcing mechanisms are out of phase and act against each other at all times. Figure 5 shows contours of the surface velocity $u|_{z=0}$ in the (t,x)-plane for the case where $S = 0.01$ and $\phi = \frac{1}{2}$. There are a number of significant differences between this case and the buoyancy only ($S = 0$) and the $\phi = 0$ cases of Figures 2 and 3. The most obvious is that for x larger than ~ 1 the surface velocity is dominated by the surface stress and is thus initially directed towards the shore against the prevailing pressure gradient. In the shallower regions near $x = 0$ the buoyancy forcing dominates and the flow is initially away from the shore, consistent with the prevailing temperature induced pressure gradient. This leads to a marked shift in the behaviour of the downwelling/upwelling fronts that emerge from the shore as the surface flow reverses. Less obvious is that the surface velocity magnitudes are generally smaller than for either of the two earlier cases. This is to be expected since in every part of the flow domain the two forcing mechanisms are in opposition.

The opposing forcing mechanisms differ in magnitude in different ways throughout the domain. This means that some parts of the domain are buoyancy dominated while in others the surface stress dominates. For example it has already been noted that for larger x surface stress dominates near the surface. The different balances in different regions lead to a complicated circulation structure particularly when the circulation is reversing. Figure 6 shows a series of streamline plots for various times as the overall circulation structure changes from nighttime to daytime conditions. For Figure 6 the buoyancy and surface stress forcing terms reversed at $t = 0.5$ so by $t = 0.75$ (Figure 6a) the forcing terms have been the same sign for 0.25 of a period and are at their highest magnitude. The regions of the domain where buoyancy and viscosity are in balance (near $x = 0$ and in the boundary layer near $z = -x$) have already established nighttime conditions with the circulation in those regions being

anticlockwise. However, for larger x and at the intermediate depths where buoyancy and unsteady inertia are in balance the circulation is clockwise due to the residual inertia of the previous period's daytime flow. Lastly, near the surface $z = 0$ where surface stress forces dominate buoyancy the circulation is again clockwise since the surface stress forcing is out of phase with the buoyancy forcing in the relatively thin surface layer. The competing processes within the flow lead to there being a stagnation point interior to the flow visible in Figure 6a at approximately $(x,z) = (6,-1)$.

By $t = 0.875$ (Figure 6b) the reversed pressure gradient has overcome the inertia of the flow in the interior of the domain with anticlockwise circulation below the dividing streamline. Above the dividing streamline the surface stress is the dominant forcing mechanism and the circulation there is clockwise.

At $t = 1.0$ (Figure 6c) both the buoyancy and surface stress forcing are zero. The circulation visible in the figure is due to the inertia of the previous flow. Below the dividing streamline the flow is anticlockwise and is the residual buoyancy forced flow while above the dividing streamline the flow is clockwise as set up by the earlier surface stress.

Figure 6d shows the circulation structure shortly after the reversal of the buoyancy conditions from nighttime to daytime conditions. As mentioned above the flow near $x = 0$ and $z = -x$ is the first to reverse with the circulation there being clockwise. In the intermediate depths the circulation is anticlockwise due to the inertia of the previous flow as well as reflecting the direction of the surface stress.

Lastly Figure 6e shows the circulation when the forcing is again at its highest magnitude but now in the opposite sense to Figure 6a. The circulation in the bulk of the domain is clockwise, reflecting established daytime conditions. There is a thin layer near the surface $z = 0$ where the surface stress dominates and the circulation there is anticlockwise. Despite Figures 6a and 6b representing equal but opposite times in the daily cycle the streamline patterns are not the same. This is because the circulation has not reached a purely periodic behaviour—it is still undergoing adjustment from the initial conditions.

Figure 7 shows a series of velocity profiles at $x = 5$ for various times as the circulation reverses for the case where $\phi = \frac{1}{2}$. There is a similar layering of the flow regimes as for Figure 4 with the flow near $z = 0$ being dominated by the surface boundary condition although in this $\phi = \frac{1}{2}$ case the flow develops differently. At $t = 0.9$ the velocity at the surface $z = 0$ is positive indicating a surface layer with clockwise circulation reflecting that direction of the surface stress. At depth where buoyancy forcing is dominant the circulation is in the opposite direction. At $t = 1$ both forcing mechanisms reverse and the flow is due to residual inertia. At $t = 1.1$ the forcing has changed direction and the surface stress dominated flow near $z = 0$ is the first to respond. As time progresses ($t = 1.1$ to 1.2) the circulation near the surface become stronger in an anticlockwise sense while the flow at depth decelerates as the buoyancy forcing increases in strength. A close inspection of the velocity profile at $t = 1.2$ shows it to have a five layer structure. By $t = 1.3$ the flow has completely reversed in response to the forcing reversal at $t = 1$ with anticlockwise circulation in the surface stress dominated region near $z = 0$ and clockwise circulation in the buoyancy dominated regions at depth.

A quantity of interest in lakes is the nett horizontal volume exchange that occurs over the daily cycle. This is calculated by integrating the absolute value of the horizontal velocity over the local depth and over one day which in dimensionless form is

$$Q_d(x,t) = \int_t^{t+1} \int_{-x}^{0} |u(x,z,\tau)|\, dz\, d\tau. \tag{27}$$

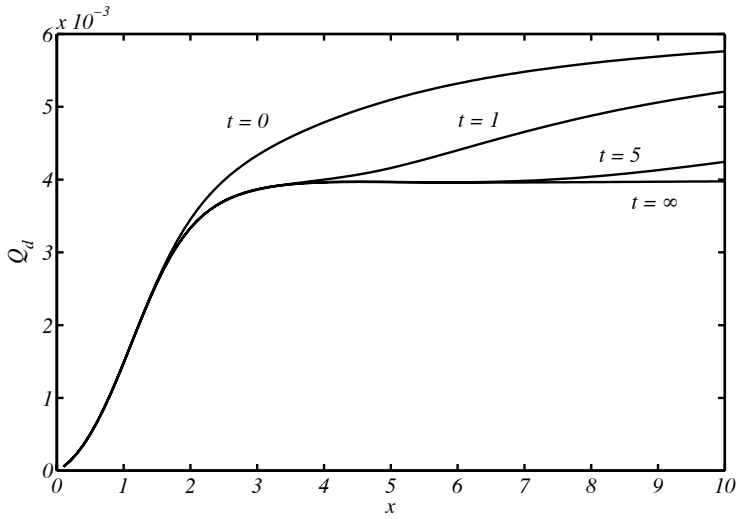

Fig. 8 Profiles of nett daily horizontal volume exchange for various times for $S = 0.01$ and $\phi = \frac{1}{2}$.

Figure 8 shows horizontal profiles of Q_d (calculated using numerical integration of (20)) at various starting times t for the $\phi = \frac{1}{2}$ case. For all times the Q_d profiles tend to zero as $x \to 0$. It can be shown that in the viscous dominated flow near $x = 0$ $Q_d \sim x^2$. In the deeper parts of the domain Q_d it takes some time of the flow to become purely periodic. Once the transient response has died away and purely periodic conditions have been established Q_d is approximately constant for large x, levelling off at approximately 4×10^{-3}.

Using $I_0 = 200\text{Wm}^{-2}$, $A = 10^{-2}$ and the usual values for the other physical parameters gives an horizontal volume exchange of approximately 10^4m^3 per unit width. At 5m depth this is equivalent to an exchange velocity of approximately 2cms^{-1}.

4 Concluding Remarks

The model for periodically forced near-shore circulation presented in this paper exhibits quite complicated behaviour despite the model being linear and using simplified forcing mechanisms. The model shows how the unsteady nature of the forcing leads to different parts of the domain having different dynamic balances. The changing balances throughout the domain lead to a complicated circulation structure, particularly as the circulation changes direction in response to reversals of the forcing. The level of complexity in the circulation is also a function of the phase difference between the two forcing mechanisms.

The model has a number of limitations that provide scope for further work. For example, the heating/cooling mechanism is vertically integrated whereas in natural lakes the heat transfer is vertically non-uniform, especially during the day [7, 10]. Another significant limitation is the absence of non-linear effects (specifically advection of heat) in the model. Further effects that are not included in the model that can be significant in natural lakes include more general topography (including three dimensional variations)and the effects of non-laminar flow. Making analytical progress for more general models is however challenging.

References

1. Cormack, D.E., Leal, L.G., Imberger, J.: Natural convection in a shallow cavity with differentially heated end walls. Part 1. asymptotic theory. J. Fluid Mech. **65**, 209–229 (1974)
2. Cormack, D.E., Leal, L.G., Seinfeld, J.H.: Natural convection in a shallow cavity with differentially heated end walls. Part 2. numerical solutions. J. Fluid Mech. **65**, 231–246 (1974)
3. Cormack, D.E., Stone, G.P., Leal, L.G.: The effect of upper surface conditions on convection in a shallow cavity with differentially heated end-walls. Intl. J. Heat Mass Transfer **18**, 635–648 (1975)
4. Farrow, D.E.: Periodically forced natural convection over slowly varying topography. J. Fluid Mech. **508**, 1–21 (2004)
5. Farrow, D.E., Patterson, J.C.: On the response of a reservoir sidearm to diurnal heating and cooling. J. Fluid Mech. **246**, 143–161 (1993)
6. Farrow, D.E., Patterson, J.C.: On the stability of the near shore waters of a lake when subject to solar heating. Int. J. Heat Mass Transfer **36**(1), 89–100 (1993)
7. Farrow, D.E., Patterson, J.C.: The daytime circulation and temperature structure in a reservoir sidearm. Int. J. Heat Mass Transfer **37**(13), 1957–1968 (1994)
8. Horsch, G.M., Stefan, H.G., Gavali, S.: Numerical simulation of colling-induced convective currents on a littoral slope. Int.. J. Numer. Meth. Fluids **19**, 105–134 (1994)
9. Imberger, J.: Natural convection in a shallow cavity with differentially heated end walls. Part 2. experimental results. J. Fluid Mech. **65**, 247–260 (1975)
10. Lei, C., Patterson, J.C.: Unsteady natural convection in a triangular enclosure induced by the absorption of radiation. J. Fluid Mech. **460**, 181–209 (2002)
11. Lei, C., Patterson, J.C.: Unsteady natural convection in a triangular enclosure induced by surface cooling. Int. J. Heat Fluid Flow **26**, 307–321 (2005)
12. Lei, C., Patterson, J.C.: Natural convection induced by diurnal heating and cooling in a reservoir with slowly varying topography. JSME Int. J. Series B **49**(3), 605–615 (2006)
13. Mao, Y., Lei, C., Patterson, J.C.: Characteristics of instability of radiation-induced natural convection in shallow littoral waters. Intl. J. Thermal Sci. **49**(1), 170–181 (2010)
14. Mao, Y., Lei, C., Patterson, J.C.: Unsteady near-shore natural convection induced by surface cooling. J. Fluid Mech. **642**, 213–233 (2010)
15. Mao, Y.D., Lei, C.W., Patterson, J.C.: Unsteady natural convection in a triangular enclosure induced by absorption of radiation - a revisit by improved scaling alnalysis. J. Fluid Mech. **622**, 74–102 (2009)
16. Monismith, S.B., Imberger, J., Morison, M.L.: Convective motions in the sidearm of a small reservoir. Limnol. Oceanogr. **35**, 1676–1702 (1990)
17. Rattray Jr., M., Hansen, D.V.: A similarity solution for circulation in an estuary. J. Marine Res. **20**, 121–133 (1962)

Acknowledgements The author would like to thank S. Brown and the anonymous reviewers for useful comments on earlier drafts of this paper.